WDM Based 10.8 Gbps Visible Light Communication with Probabilistic Shaping

Tilahun Zerihun Gutema, *Student Member, IEEE,* Harald Haas, *Fellow, IEEE,* and Wasiu O. Popoola, *Senior Member, IEEE*

***Abstract*—In this work, we study probabilistic shaping (PS) for optical wireless communications and apply the technique to wavelength division multiplexing (WDM) based visible light communication (VLC). The performance of the proposed scheme is validated with an experimental demonstration. The experimental set up uses lenses to collimate the light beam for triple LEDs. The system parameters of the WDM based VLC system are then optimised, the channel response measured, and PS based symbols are allocated to the individual orthogonal frequency division multiplexing (OFDM) subcarriers. For the channel conditions under consideration, PS resulted in a near Shannon capacity transmission rate of 10.81 Gb/s. Comparatively, the PS resulted in 25 % higher transmission rate than the widely used adaptive bit-power loading algorithm under the same channel conditions.**

***Index Terms*—Probabilistic shaping (PS), adaptive bit-power loading, orthogonal frequency division multiplexing (OFDM), visible light communication (VLC), light fidelity (LiFi), wavelength division multiplexing (WDM).**

I. Introduction

VISIBLE light communication (VLC), based on light-emitting diodes (LEDs), is an emerging optical wireless communication (OWC) technology that operates in the visible light spectrum and leverages the existing lighting infrastructures for communication. Additionally, energy-efficient, low cost and widely available front-end devices enable VLC to attract increasing interest for indoor wireless connectivity [1], [2].

Despite a huge unlicensed optical spectrum, the −3 dB modulation bandwidth of commercially available LEDs is limited to only a few MHz [2], [3]. Moreover, the overall frequency response of a VLC system is frequency-selective due to the limited modulation bandwidth of LEDs and front-end devices [4], [5]. Hence, for high-speed VLC, it is incumbent to operate beyond the −3 dB modulation bandwidth of LEDs. This can be achieved by implementing appropriate signal processing techniques at the transmitter and/or the receiver such as precoding and equalisation [6], [7]. Orthogonal frequency division multiplexing (OFDM) is a convenient modulation scheme for this as it offers efficient use of the available spectrum and it is robust against channel frequency selectivity [8]. It also allows for low-complexity single-tap equalisers in the frequency domain. Most prominently, it enables allocation of bits and power on the individual subcarrier, depending on the frequency response/gain per subcarrier of the communication link [3]. This has led to high data rate transmissions using a single LED [3], [9], [10]. A wavelength division multiplexing (WDM) based VLC has also been explored for higher data rates in [11]–[13]. All these studies consider adaptive bit loading with OFDM. In adaptive bit-power loading, discrete integer level bits per symbol are allocated onto each subcarrier. But this does not provide the best possible fit to the channel frequency response. Thus, there still exists a capacity gap to the channel capacity limit as formulated by Shannon [14].

A data rate close to the capacity of an additive white Gaussian noise (AWGN) channel, under the power constraint of a transmitter, can be realised when the channel is fed by a Gaussian source [15]. This can be attained by applying a probabilistic shaping (PS) to quadrature amplitude modulation (QAM) symbols, which gives a Gaussian-like distribution over the input constellation [16]. Thus, low energy symbols are transmitted more frequently than high energy symbols. Consequently, in PS, data symbols are no longer uniformly distributed but are assigned different probabilities of occurrence. This is realised by using a distribution matcher, such as constant composition distribution matcher (CCDM), proposed in [17]. The distribution matcher maps input bits into non-equiprobable symbols with the desired distribution. As such, with PS, continuous entropy allocation is possible to utilise the available bandwidth efficiently [18].

There are some efforts toward using PS to enhance the achievable information rate (AIR) of a single LED based VLC system. Error performance of a DC-biased optical OFDM communication system employing PS and uniformly distributed symbols is presented through Monte Carlo simulations in [19]. In [20], a single LED VLC with PS based OFDM is reported. However, despite the channel's capacity to accommodate higher modulation orders, the work is limited to the PS with 256-QAM (PS-256-QAM).Besides, subcarriers that are assigned to a group with the same QAM modulation order in the bit-loading scheme, are allocated with the same entropy in PS-256-QAM. This is contrary to the continuous

This work was supported by the European Union's Horizon 2020 research and innovation programme under the Marie Skłodowska Curie grant agreement №. 814215 titled ENLIGHT'EM: European Training Network in Low-Energy Visible Light IoT Systems [Online]. Available: https://enlightem.eu/. *(Corresponding author: Tilahun Zerihun Gutema).*

Tilahun Zerihun Gutema and Wasiu O. Popoola are with the Institute for Digital Communications, School of Engineering, The University of Edinburgh, Edinburgh, EH9 3FD, UK (e-mail: tilahun.gutema@ed.ac.uk; w.popoola@ed.ac.uk).

Harald Haas is with University of Strathclyde, The Technology and Innovation Centre, 99 George Street, Glasgow, G1 1RD, U.K. (e-mail: harald.haas@strath.ac.uk).

Color versions of one or more figures in this article are available at https://doi.org/10.1109/JLT.2022.3175575.

Digital Object Identifier 10.1109/JLT.2022.3175575

entropy allocation that should fit the channel SNR response. A laser diode (LD)-based underwater OWC applying OFDM with PS-256-QAM has also been demonstrated to improve transmission capacity in [21]. A similar approach with LD-based VLC system using higher-order format (PS-1024-QAM) is also reported in [22].

In this work, we demonstrate in an experiment a WDM based VLC system with PS and OFDM. The demonstration uses three (red, green, and blue) off-the-shelf LEDs. In the experiment, the PS is validated and compared with the bit-power loading scheme. Our results show that with PS, the capacity can be increased by over 25 % compared to the bit-power loading approach.

The remainder of the paper is organised as follows. In Section II, the framework of PS and the principle of adaptive entropy loading using PS in optical OFDM is discussed. In Section III, the experimental demonstration of PS in WDM based VLC system is presented. Finally, concluding remarks are provided in Section IV.

II. System Description and Performance Analysis

In this section, the basics of generating PS QAM symbols is presented. The principle of adaptive entropy loading employing PS for optical OFDM is also detailed.

A. Probabilistic Shaped QAM Signal

An M-QAM symbol can be represented by its in-phase and quadrature components. In each symbol interval, T_{s}, these information-bearing signal amplitudes are chosen independently from a set comprising $\left\{2i-1-\sqrt{M}\right\}$, $i = 1, 2, \cdots, \sqrt{M}$. For a square M-QAM, where $\log_2 M$ is even, its constellation is therefore composed of two orthogonal pulse-amplitude modulation ($\sqrt{M}$-PAM) constellations. This means that every QAM symbol can be considered as two PAM symbols with constellation points taken from $\chi = \left\{x_1, x_2, \cdots, x_{\sqrt{M}}\right\}$. In PS, a common approach to maximise the channel capacity is to use shaped input distribution from the family of Maxwell-Boltzmann (MB) distribution [15], [23]. For $\sqrt{M}$-PAM, the corresponding MB distribution probability mass function (PMF) $P_X(x_i)$ can be written as:

$$P_X(x_i) = \frac{1}{\sum_{j=1}^{\sqrt{M}} \mathrm{e}^{-\lambda |x_j|^2}} \mathrm{e}^{-\lambda |x_i|^2}, \tag{1}$$

where λ is a rate parameter used to search for the optimum PMF that maximises capacity. Note that, the PMF becomes uniform distribution when $\lambda = 0$ and as λ increases, the constellation distribution becomes Gaussian with reduced variance. The PMF of the M-QAM constellation is the product of the respective constituent PAM probabilities. To illustrate, Fig. 1 shows the PMF of PS-8-PAM with $\lambda = 0.0408$ and the corresponding PS-64-QAM distribution.

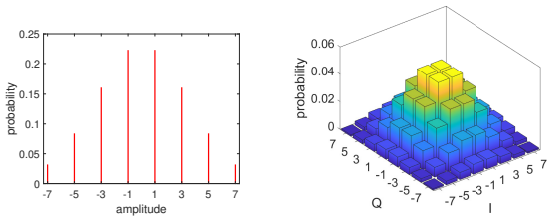

(a) PMF of PS-8-PAM (b) PMF of PS-64-QAM

Fig. 1. Graphical illustration of PS-64-QAM generated from its one dimensional constitute PS-8-PAM with $\lambda = 0.0408$.

B. Adaptive Entropy Loading for Optical OFDM

Various forms of OFDM modulation schemes have been proposed for VLC [8]. These modulation techniques should satisfy the requirement of intensity modulation (IM) to generate real and unipolar LED modulating signal. A DC-biased optical OFDM (DCO-OFDM) is one of the most widely used spectrally efficient optical OFDM modulation schemes. In DCO-OFDM, a direct current bias is added to generate a unipolar signal. Furthermore, to realise real-valued OFDM waveform, Hermitian symmetry is imposed on the subcarriers of the OFDM frames such that $X[k] = X^*[N_{\mathrm{FFT}} - k]$ and $X[0] = X[N_{\mathrm{FFT}}/2] = 0$ where N_{FFT} is the number of subcarriers, and k is the subcarrier index [24], [25].

The response of a VLC channel is frequency-selective which due to the limited modulation bandwidth of LEDs, and the channel itself [5]. Consequently, different subcarriers/subbands have different SNR values. Applying a fixed-rate OFDM by allocating QAM signal with a fixed modulation order, to all subcarriers leads to underestimating the channel capacity [9]. Alternatively, the entropy of the system should be allocated adaptively for each subcarrier in order to maximise the AIR. This is attained by estimating the available SNR of each subcarrier, SNR_k, prior to the actual data transmission. In the following subsections, the principles of entropy allocation using the adaptive bit-power loading and PS as well as performance comparison metrics are presented.

1) Adaptive bit-power loading based optical OFDM: In the bit-power loading scheme, the estimated SNR_k is used to adaptively assign the subcarriers with different QAM formats. It allows for higher modulation orders to be used in the subcarriers with higher estimated SNR. This is achieved while ensuring the target probability of error, P_b^{T} is below the forward error correction (FEC) limit of 3×10^{-3}. The adaptive bit-power loading which is based on the Levin-Campello algorithm [26], involves the following optimisation on each OFDM subcarrier:

$$\text{maximise} \quad m_k = \log_2 M_k \tag{2a}$$

$$\text{subject to} \quad \mathrm{BER}(M_k, \mathrm{SNR}_k) \leq P_b^{\mathrm{T}} \tag{2b}$$

$$\sum_{k=1}^{\frac{N_{\mathrm{FFT}}}{2}-1} \nu_k^2 = N_{\mathrm{act}}. \tag{2c}$$

Here, m_k is the number of bits/symbol per subcarrier, N_{act} is the number of active data subcarriers with $m_k > 2$ bits/symbol, ν_k^2 is the power loading factor, and $\mathrm{BER}(M_k, \mathrm{SNR}_k)$ given by (3) [27], is the theoretical BER of M_k-QAM for subcarrier k

with SNR_k.

$$\mathrm{BER}\left(M_k, \mathrm{SNR}_k\right) \approx \frac{4}{\log_2 M_k}\left(1-\frac{1}{\sqrt{M_k}}\right) \times \sum_{l=1}^{2} Q\left((2l-1)\sqrt{\frac{3\mathrm{SNR}_k}{M_k-1}}\right). \quad (3)$$

Here, $Q(\cdot)$ denotes the Gaussian Q-function.

2) PS Based Optical OFDM: The adaptive bit-power loading technique applies discrete integer level bit allocation onto each subcarrier which is not a perfect fit for the channel frequency response. However, PS based entropy loading can provide a better fit to the channel response and thus approach the channel capacity limit [28]. For PS based optical OFDM scheme, different probabilistic constellation distributions with a fixed modulation order, M-QAM symbols are applied to individual subcarriers based on the pre-estimated SNR. Assuming that the PS-M-QAM constellation points are taken from $\chi = \{x_1, x_2, \cdots, x_M\}$ with PMF $P_X(x_i)$, and a channel capacity C_k, this optimisation process can be expressed as follows:

$$\text{minimise} \quad \left| -\sum_{\substack{i=1,\\ x_i \in \chi}}^{M_k} P_X(x_i)\log_2 P_X(x_i) - C_k \right| \quad (4a)$$

$$\text{subject to} \quad C_k = \log_2\left(1+\mathrm{SNR}_k\right). \quad (4b)$$

In this work, the constant composition distribution matcher (CCDM), proposed in [17], is utilised to map input information bits to probabilistically shaped symbols and realise the above optimisation process. A square PS-M-QAM signal is generated by using two orthogonal $\sqrt{M}$-PAM symbols that represent real and imaginary parts of the M-QAM symbol as discussed in section II-A.

C. Generalised Mutual Information

Generalised mutual information (GMI) is an effective performance metrics to accurately represent the achievable information rate of a system with ideal binary soft-decision (SD) decoding [29], [30]. Moreover, normalised GMI (NGMI) is regarded as a reliable SD-FEC threshold for uniform as well as for probabilistically shaped QAM, which is given by NGMI = $1-(H-\mathrm{GMI})/\log_2 M$, where H represents the entropy of PS-M-QAM [29]. For uniform M-QAM, $H = m = \log_2 M$ [29]. The required amount of ideal FEC overhead (OH) to achieve error-free post-FEC can also be inferred from the NGMI using $(1-\mathrm{NGMI})/\mathrm{NGMI}$ [20]. For a multicarrier system, which is the focus of this work, the average NGMI is used. Therefore, GMI and NGMI can be used to compare the transmission capacity performance and the required FEC OH for both uniform M-QAM and PS-M-QAM.

For an auxiliary AWGN channel with independent and identically distributed discrete input, $X = [X_1, X_2, \cdots, X_N]$ and the corresponding output, $Y = [Y_1, Y_2, \cdots, Y_N]$, the GMI can be calculated through Monte Carlo simulations of N samples as [23]:

$$\mathrm{GMI} \approx \frac{1}{N}\sum_{n=1}^{N}\left[-\log_2 P_X(x_n)\right] - \frac{1}{N}\sum_{n=1}^{N}\sum_{i=1}^{m}\left[\log_2\left(1+\mathrm{e}^{(-1)^{b_{n,i}}\Lambda_{n,i}}\right)\right], \quad (5)$$

where the first term in (5) is the entropy of the constellation, and the second term calculates the impact of channel noise from measured channel statistics and the probabilistic distributions. $b_{n,i} \in \{0,1\}$ is the i^{th} bit of the n^{th} transmit symbol, and the soft bit-wise demapper output $\Lambda_{n,i}$, are the log-likelihood ratios (LLRs) computed with 2D Gaussian auxiliary channel as [23]:

$$\Lambda_{n,i} = \log\frac{\sum_{x\in\chi_1^i}\mathrm{e}^{-\frac{|y_k-x|^2}{2\sigma^2}}P_X(x)}{\sum_{x\in\chi_0^i}\mathrm{e}^{-\frac{|y_k-x|^2}{2\sigma^2}}P_X(x)}, \quad (6)$$

where χ_1^i and χ_0^i denote the set of constellation points whose i^{th} bit is 1 or 0, respectively. σ^2 is the noise variance of the AWGN channel.

Once the GMI of each subcarrier is evaluated from the measured channel statistics and the distributions of the received symbols using (5), the overall data rate of the VLC system is obtained as:

$$R_{\mathrm{b}} = \frac{\sum_{k=1}^{\frac{N_{\mathrm{FFT}}}{2}-1}\mathrm{GMI}_k}{N_{\mathrm{FFT}}+N_{\mathrm{CP}}} \times R_{\mathrm{s}}, \quad (7)$$

where R_{s} is the symbol rate, and N_{CP} is the cyclic prefix size. Note that the data rate in (7) is an aggregate data rate before removing the FEC OH and we assume an ideal FEC.

III. Experimental Demonstration

This section details the experimental setup and results that demonstrate the performance comparison of adaptive bit-power loading and PS in a WDM based VLC system.

A. Experimental Setup

The system block diagram along with the picture of the setup in the lab is shown in Fig. 2. The signal generation and detection process of DCO-OFDM is implemented in MATLAB. In the transmitter side, a stream of binary input is generated and then mapped into M-QAM symbols. In the bit-power loading scheme, different QAM formats are applied at each subcarrier based on the pre-estimated SNR. For the PS based OFDM system, a fixed M-QAM with different probabilistic constellation distributions is applied. Hermitian symmetry is imposed, and each symbol is loaded into orthogonal subcarriers by applying an inverse fast Fourier transform (IFFT). The OFDM frame size is set to $N_{\mathrm{FFT}} = 2048$ subcarriers. Cyclic prefixes (CPs) are inserted at the start of each OFDM frame. A value of $N_{\mathrm{CP}} = 5$ is found to be sufficient for the intersymbol interferes (ISI) to be removed [10], [31]. The symbols can then be multiplexed into serial time-domain output. The waveform pattern is then uploaded to an arbitrary waveform generator (AWG: Keysight M8195A). The sampling rate of the AWG is set to 16 GSa/s. Note

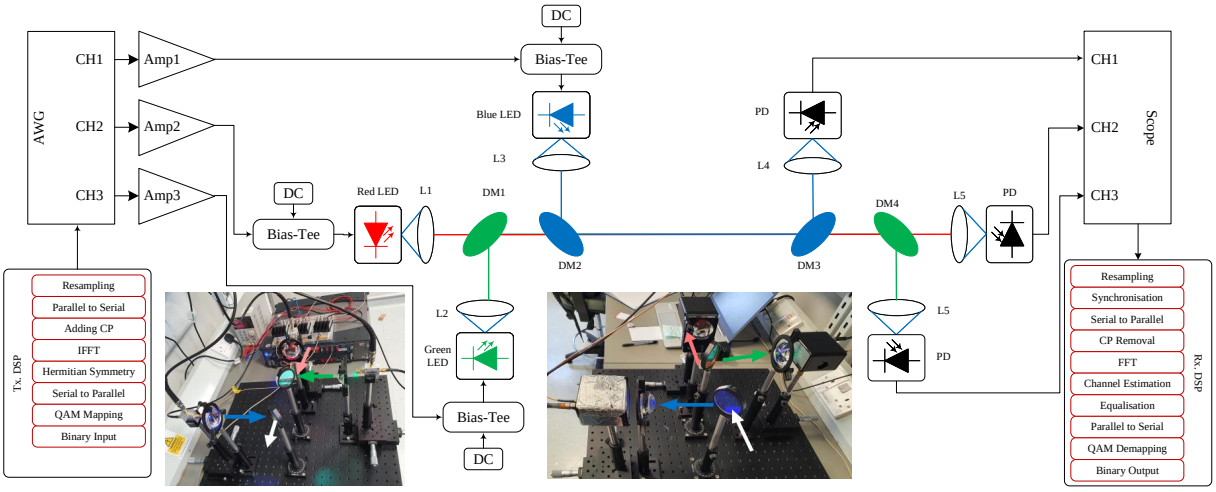

Fig. 2. Experimental setup with the picture of the set-up at the transmitter and receiver sides, and signal generation and detection DSP steps.

that the modulating signals, for the three colours, are generated using different seeds and are thus independent of each other. Each output signal from the AWG is amplified (Amp1, Amp2, Amp3: Mini-Circuits ZHL-1A-S+) and fed into Bias-Tees (Mini-Circuits ZFBT-4R2GW+) which superimpose the OFDM signal with the DC bias current. Each bias-tee output is used to drive off-the-shelf red, green, and blue (598-8D10-107F, 598-8081-107F, 598-8D90-107F) micro-LEDs which have dominant wavelengths of 630 nm, 525nm, and 470nm, respectively. Since the half-power semi-angles of the LEDs are wide (i.e. about 70°), aspherical condenser lenses (L1, L2, L3: Thorlabs ACL4532) are used to collimate the output light from individual transmitters. The modulated output signals of all three colours of LEDs are combined with dichroic mirrors as shown in Fig. 2. The first dichroic mirror (DM1: Thorlabs DMLP605L), which has a 620 - 800 nm transmission band and 605 nm cut-on wavelength, transmits red while reflecting the green signal. Another dichroic mirror (DM2: Thorlabs DMLP490L), with 505 - 800 nm transmission band and 490 nm cut-on wavelength, passes red and green while reflecting the blue signal. At this level, a combination of the red, green, and blue collimated light signal is attained.

The receiver is 50 cm away from the transmitter. It consists of the same configuration of dichroic mirrors to separate and send each colour to its respective photoreceiver. One dichroic mirror (DM3: Thorlabs DMLP490L) reflects the blue light while the other (DM4: Thorlabs DMLP605L) separates the green. Aspherical condenser lenses (L4, L5, L6: Thorlabs ACL50832) are used to focus the light into the active detection area of photodetectors (PD: New Focus 1601 AC). The receiver has a −3 dB bandwidth of 1 GHz and a built-in transimpedance amplifier (TIA) with a gain of 700 V/A. The output signal of each receiver is captured by using the three channels of a high-speed oscilloscope (OSC: Keysight MSO7104B) sampling at 4 GSa/s and followed by signal processing in MATLAB. The received waveform from the oscilloscope is resampled and symbols synchronised. The CPs are then removed and the symbols demodulated.

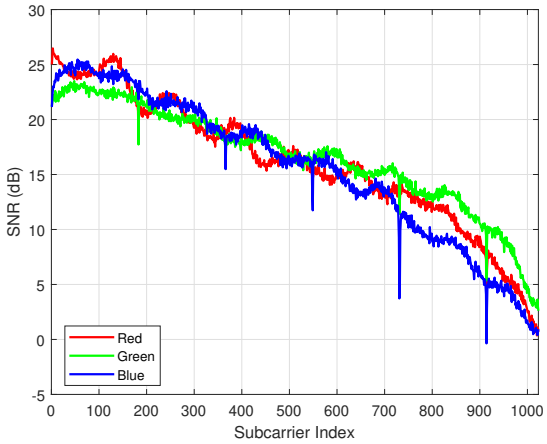

Fig. 3. Channel SNR response versus individual subcarriers for the red, green, and blue links at the optimum DC bias and Vpp.

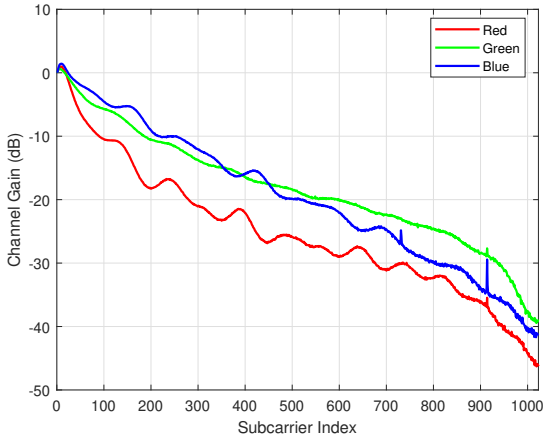

Fig. 4. Channel gain versus individual subcarriers for the red, green, and blue links at the optimum DC bias and Vpp.

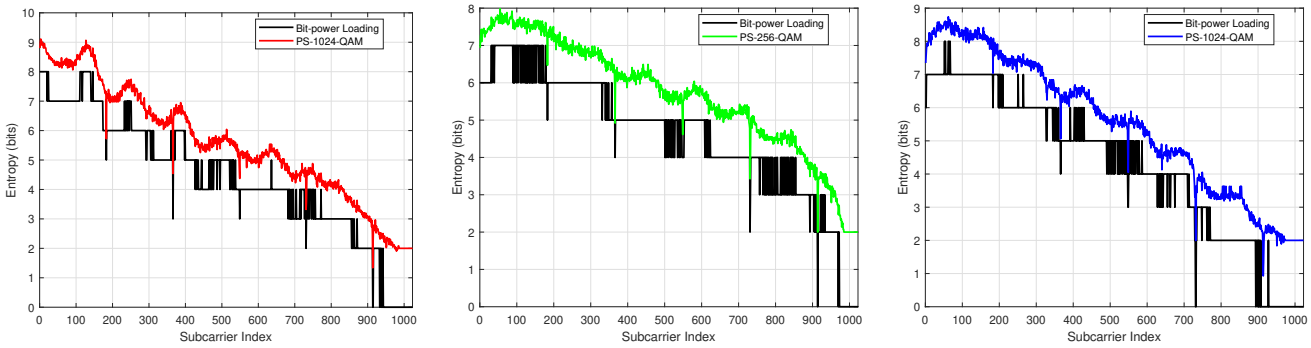

(a) Red (b) Green (c) Blue

Fig. 5. Entropy allocation per subcarrier in PS and bit-power loading for red, green, and blue links.

In the experiment, the channel response and available SNR of each subcarrier, SNR_k, are estimated using pilots composed of multiple 4-QAM based OFDM frames. The SNR for each OFDM subcarrier is obtained by evaluating the error vector magnitude (EVM) of the received pilot 4-QAM signal [32]. Note that, in PS based OFDM, 1024-QAM symbols are mapped into individual subcarriers for the red and blue links while 256-QAM is used in the green link. The PS-M-QAM symbols are generated from two orthogonal $\sqrt{M}$-PAM symbols. The choice of this higher modulation order allows utilising the available channel to the full extent. However, it comes with a requirement of a greater number of sample points which goes beyond the memory depth of the available oscilloscope. Consequently, the GMI performance of PS based system is evaluated offline from experimentally measured channel response. To carry out a fair comparison, this offline performance measurement is repeated to the bit-power loading technique and used to make a comparison with the PS technique.

B. Experimental Results and Discussions

The WDM VLC data transmission is performed at a symbol rate, R_s = 1.4 GBaud. The DC bias point of the LEDs is a significant parameter of the experiment. For each LED, the optimum driving point is determined by minimising the possible signal distortion while the information bits to be loaded is maximised. Details of the DC bias optimisation process can be found in [33]. Accordingly, the DC bias of the red, green, and blue LEDs are found as 45 mA, 50 mA, 45 mA at which the −3 dB modulation bandwidths are 22 MHz, 32.4 MHz, and 51.5 MHz, respectively. Through an iterative process, the optimum values of modulating signal amplitude which maximise the SNR responses of the red, blue, and green LED links are found to be 450 mVpp, 350 mVpp, and 200 mVpp, respectively.

Fig. 3 shows the overall SNR response of the system per subcarrier index at these optimum DC bias point and Vpp. For all measurements, SNR drop is observed at some subcarrier index due to nonlinear harmonic distortion in the system. Despite reducing the number of bits that could be loaded onto these subcarriers, it does not affect the system error performance as bits are allocated based on the estimated SNR. All the links exhibit comparable SNR responses in all frequency ranges.

The overall frequency response in terms of the channel gain of the system for each colour is also presented in Fig. 4. The amount of optical power detected by individual photodetectors is important to the channel gain. Even though the amount of optical cross-talk is found to be minimal, a substantial portion of power is lost due to the dichroic mirrors. The optical power detected by the red, green, and blue receivers with the dichroic mirrors in the setup is found to be only 91 %, 89 %, and 95 % of the setup without the dichroic mirrors, respectively.

The adaptive bit allocated per subcarrier and the rate used in the PS schemes for each of the links is shown in Fig. 5. The entropy of the bit-power loading system takes only discrete integers. For red, green, and blue links a maximum of 8 bit/symbol, 7 bit/symbol, and 8 bit/symbol are allocated. Besides, for red, green, and blue links 902, 953, and 857 data subcarriers, respectively, are loaded with at least two or more bit/symbol. The PS scheme is set to take continuous entropy values equal to the corresponding channel capacities. A fixed 1024-QAM signal level is applied in all subcarriers to both red and blue links, as these links can have above 8 bit/symbol entropy. Meanwhile, the green link can allocate just below 8 bit/symbol with which 256-QAM is employed.

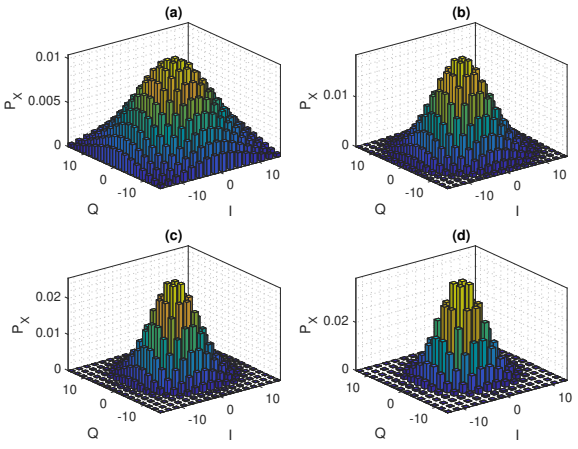

Fig. 6. Graphical illustration of PS-256-QAM signal employed to the green link with four different entropy values at subcarrier index of (a) 100 (b) 200 (c) 300 and (d) 400.

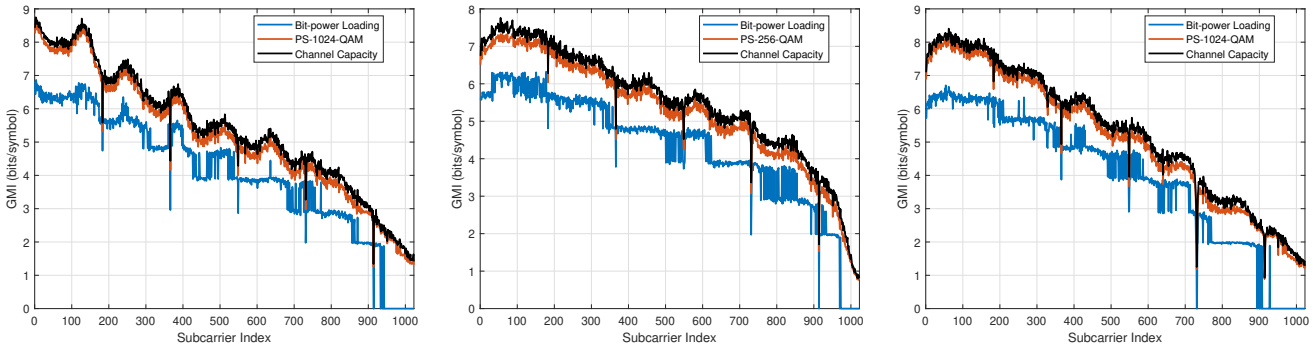

(a) Red (b) Green (c) Blue

Fig. 7. Measured GMI per subcarrier in PS and bit-power loading based OFDM schemes for red, green, and blue links.

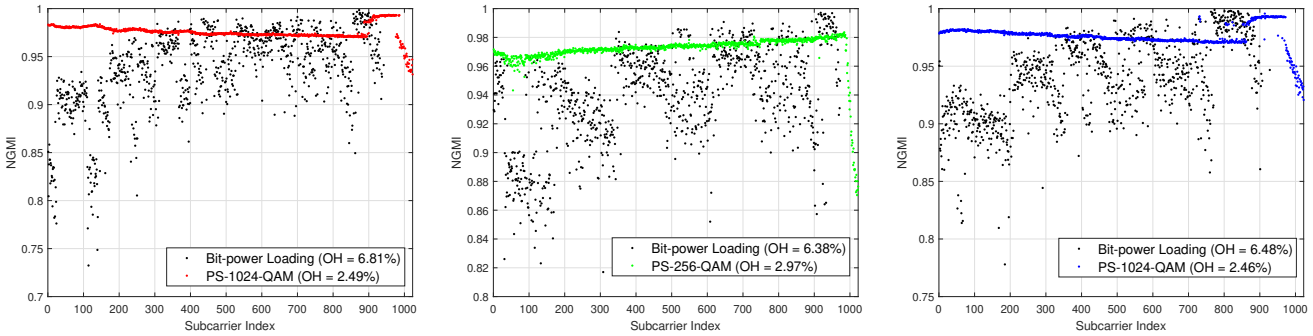

(a) Red (b) Green (c) Blue

Fig. 8. NGMI per subcarrier in PS and bit-power loading based OFDM schemes for red, green, and blue links.

The graphical illustration of the PS-256-QAM signal employed to the green link at four different subcarriers is shown in Fig. 6. For the higher subcarriers, the distribution becomes becomes Gaussian with reduced variance since the entropy decrease, and the probability of occurrence of outer point may also converge to zero.

The performance of the bit-power loading and PS schemes is analysed by evaluating the GMI values in each of the colours. These GMI results at different subcarriers applying bit-power loading and PS are shown in Fig. 7 for each colour. The GMI of Shannon's channel capacity of each link based on additive white Gaussian noise (AWGN) channel is also presented as a reference. In all three links, the PS based OFDM technique approaches Shannon's capacity, while the bit-power loading exhibits a gap to the capacity limit across all subcarriers. The NGMI result per subcarrier for each colour is also shown in Fig. 8. The PS has the highest and almost consistent NGMI values with average NGMI = {0.9757, 0.9712, 0.9760} while for the bit-power loading the average NGMI = {0.9362, 0.9400, 0.9391} for the red, green, and blue links, respectively. The corresponding FEC OH requirement in each scheme for each colours is shown in Table I.

In terms of data rate, in PS, an aggregate data rate of 10.81 Gb/s is achieved. This is only with under 3 % overall FEC OH requirement. The aggregate net data rate after the FEC OH reductions in each colour is 10.52 Gb/s. Meanwhile, using bit-power loading, only 8.60 Gb/s aggregate data rate with approximately 7 % overall FEC OH requirement is attained. The net data rate after the FEC OH reduction is 8.04 Gb/s. The summary of data rates achieved in each scheme for each colour is shown in Table I. The result indicates that PS improves the capacity by almost 25.7 % (which is about 30.8 % if the net data rate is considered) compared with the bit-power loading scheme and with a lower FEC overhead requirement. At the same FEC overhead of 3 %, the gain is even higher at over 45.1 %. These results clearly demonstrate that the VLC information rate can be enhanced substantially with the application of PS and WDM.

TABLE I
SUMMARY OF DATA RATE AND FEC OH RESULTS

	Data Rate (Gb/s)		FEC OH (%)		Net Rate (Gb/s)	
	BPL	PS	BPL	PS	BPL	PS
Red	2.84	3.61	6.81	2.49	2.65	3.52
Green	2.99	3.65	6.38	2.97	2.80	3.54
Blue	2.77	3.55	6.48	2.46	2.59	3.46
Aggregate	8.60	10.81	—		8.04	10.52

IV. CONCLUSION

In this work, we have studied probabilistic shaping for WDM based VLC systems by independently modulating three LEDs of different colours for parallel and simultaneous data transmission. The proposed scheme is validated with an experimental demonstration whereby the output light of LEDs

is collimated using lenses to focus the incident optical power on the respective photodetectors. Unlike the bit-power loading optimisation method, PS provides continuous entropy loading that makes efficient use of the available bandwidth well beyond the −3 dB point. The PS scheme results in an aggregate AIR of 10.81 Gbps, a 25.7 % increase over the bit-power loading approach. The results demonstrate that PS can be utilised to closely approach the VLC system capacity and maximise the achievable information rate.

ACKNOWLEDGMENT

For the purpose of open access, the authors have applied a Creative Commons Attribution (CC BY) licence to any Author Accepted Manuscript version arising from this submission.

REFERENCES

[1] D. Karunatilaka, F. Zafar, V. Kalavally, and R. Parthiban, "LED based indoor visible light communications: State of the art," *IEEE Communications Surveys & Tutorials*, vol. 17, no. 3, pp. 1649–1678, 2015.

[2] Z. Ghassemlooy, W. Popoola, and S. Rajbhandari, *Optical wireless communications: system and channel modelling with MATLAB®*. CRC press, 2019.

[3] A. Khalid, G. Cossu, R. Corsini, P. Choudhury, and E. Ciaramella, "1-Gb/s transmission over a phosphorescent white LED by using rate-adaptive discrete multitone modulation," *IEEE Photonics Journal*, vol. 4, no. 5, pp. 1465–1473, 2012.

[4] G. Egecan, K. Akande, P. A. Haighy, and W. Popoola, "Frequency response modelling of cool and warm white LEDs in VLC systems," in *Proceedings of the First Western Conference on Wireless Telecommunications Western Asia, Isfahan, Iran*, 2017.

[5] M. M. Mohammed, C. He, and J. Armstrong, "Performance analysis of ACO-OFDM and DCO-OFDM using bit and power loading in frequency selective optical wireless channels," in *2017 IEEE 85th Vehicular Technology Conference (VTC Spring)*. IEEE, 2017, pp. 1–5.

[6] H. Ma, L. Lampe, and S. Hranilovic, "Robust MMSE linear precoding for visible light communication broadcasting systems," in *2013 IEEE Globecom Workshops (GC Wkshps)*. IEEE, 2013, pp. 1081–1086.

[7] D. Tsonev, S. Videv, and H. Haas, "Unlocking spectral efficiency in intensity modulation and direct detection systems," *IEEE Journal on Selected Areas in Communications*, vol. 33, no. 9, pp. 1758–1770, 2015.

[8] M. S. Islim and H. Haas, "Modulation techniques for LiFi," *ZTE communications*, vol. 14, no. 2, pp. 29–40, 2019.

[9] D. Tsonev, H. Chun, S. Rajbhandari, J. J. McKendry, S. Videv, E. Gu, M. Haji, S. Watson, A. E. Kelly, G. Faulkner *et al.*, "A 3-Gb/s single-LED OFDM-Based wireless VLC link using a Gallium Nitride μLED," *IEEE Photonics Technology Letters*, vol. 26, no. 7, pp. 637–640, 2014.

[10] M. S. Islim, R. X. Ferreira, X. He, E. Xie, S. Videv, S. Viola, S. Watson, N. Bamiedakis, R. V. Penty, I. H. White *et al.*, "Towards 10 Gb/s orthogonal frequency division multiplexing-based visible light communication using a gan violet micro-LED," *Photonics Research*, vol. 5, no. 2, pp. A35–A43, 2017.

[11] R. Bian, I. Tavakkolnia, and H. Haas, "15.73 Gb/s visible light communication with off-the-shelf leds," *Journal of Lightwave Technology*, vol. 37, no. 10, pp. 2418–2424, 2019.

[12] H. Chun, S. Rajbhandari, G. Faulkner, D. Tsonev, E. Xie, J. J. D. McKendry, E. Gu, M. D. Dawson, D. C. O'Brien, and H. Haas, "LED based wavelength division multiplexed 10 Gb/s visible light communications," *Journal of lightwave technology*, vol. 34, no. 13, pp. 3047–3052, 2016.

[13] F. Wu, C.-T. Lin, C. Wei, C. Chen, Z. Chen, H. Huang, and S. Chi, "Performance comparison of OFDM signal and cap signal over high capacity rgb-led-based wdm visible light communication," *IEEE Photonics Journal*, vol. 5, no. 4, pp. 7 901 507–7 901 507, 2013.

[14] C. E. Shannon, "A mathematical theory of communication," *Bell system technical journal*, vol. 27, no. 3, pp. 379–423, 1948.

[15] F. R. Kschischang and S. Pasupathy, "Optimal nonuniform signaling for gaussian channels," *IEEE Transactions on Information Theory*, vol. 39, no. 3, pp. 913–929, 1993.

[16] F. Buchali, F. Steiner, G. Böcherer, L. Schmalen, P. Schulte, and W. Idler, "Rate adaptation and reach increase by probabilistically shaped 64-qam: An experimental demonstration," *Journal of Lightwave Technology*, vol. 34, no. 7, pp. 1599–1609, 2016.

[17] P. Schulte and G. Böcherer, "Constant composition distribution matching," *IEEE Transactions on Information Theory*, vol. 62, no. 1, pp. 430–434, 2015.

[18] T. Z. Gutema and W. O. Popoola, "Single LED Gbps visible light communication with probabilistic shaping," in *GLOBECOM 2021-2021 IEEE Global Communications Conference*. IEEE, 2021, pp. 1–6.

[19] T. Z. Gutema, H. Haas, and W. O. Popoola, "OFDM based visible light communication with probabilistic shaping," in *Proceedings of the Workshop on Light Up the IoT*, 2020, pp. 1–5.

[20] C. Xie, Z. Chen, S. Fu, W. Liu, Z. He, L. Deng, M. Tang, and D. Liu, "Achievable information rate enhancement of visible light communication using probabilistically shaped OFDM modulation," *Optics express*, vol. 26, no. 1, pp. 367–375, 2018.

[21] X. Hong, C. Fei, G. Zhang, and S. He, "Probabilistically shaped 256-QAM-OFDM transmission in underwater wireless optical communication system," in *2019 Optical Fiber Communications Conference and Exhibition (OFC)*. IEEE, 2019, pp. 1–3.

[22] G. Li, F. Hu, P. Zou, C. Wang, G.-R. Lin, and N. Chi, "Advanced Modulation Format of Probabilistic Shaping Bit Loading for 450-nm GaN Laser Diode based Visible Light Communication," *Sensors*, vol. 20, no. 21, p. 6143, 2020.

[23] T. Fehenberger, A. Alvarado, G. Böcherer, and N. Hanik, "On probabilistic shaping of quadrature amplitude modulation for the nonlinear fiber channel," *Journal of Lightwave Technology*, vol. 34, no. 21, pp. 5063–5073, 2016.

[24] J. Armstrong, "OFDM for optical communications," *Journal of lightwave technology*, vol. 27, no. 3, pp. 189–204, 2009.

[25] J. B. Carruthers and J. M. Kahn, "Multiple-subcarrier modulation for nondirected wireless infrared communication," *IEEE Journal on Selected Areas in Communications*, vol. 14, no. 3, pp. 538–546, 1996.

[26] H. E. Levin, "A complete and optimal data allocation method for practical discrete multitone systems," in *GLOBECOM'01. IEEE Global Telecommunications Conference (Cat. No. 01CH37270)*, vol. 1. IEEE, 2001, pp. 369–374.

[27] F. Xiong, *Digital modulation techniques*, 2nd ed. Artech House Publishers, 2000.

[28] D. Che and W. Shieh, "Squeezing out the last few bits from band-limited channels with entropy loading," *Optics express*, vol. 27, no. 7, pp. 9321–9329, 2019.

[29] J. Cho, L. Schmalen, and P. J. Winzer, "Normalized generalized mutual information as a forward error correction threshold for probabilistically shaped QAM," in *2017 European Conference on Optical Communication (ECOC)*. IEEE, 2017, pp. 1–3.

[30] A. Alvarado, E. Agrell, D. Lavery, R. Maher, and P. Bayvel, "Replacing the soft-decision FEC limit paradigm in the design of optical communication systems," *Journal of Lightwave Technology*, vol. 33, no. 20, pp. 4338–4352, 2015.

[31] D. Tsonev, S. Videv, and H. Haas, "Towards a 100 Gb/s visible light wireless access network," *Optics express*, vol. 23, no. 2, pp. 1627–1637, 2015.

[32] R. A. Shafik, M. S. Rahman, and A. R. Islam, "On the extended relationships among EVM, BER and SNR as performance metrics," in *2006 International Conference on Electrical and Computer Engineering*. IEEE, 2006, pp. 408–411.

[33] T. Z. Gutema, H. Haas, and W. O. Popoola, "Bias point optimisation in LiFi for capacity enhancement," *Journal of Lightwave Technology*, vol. 39, no. 15, pp. 5021–5027, 2021.

Tilahun Zerihun Gutema (Student Member, IEEE) received his B.Sc. degree in electrical engineering from Addis Ababa University, Addis Ababa, Ethiopia in 2015, and M.Sc. degree in optics and photonics, from Karlsruhe Institute of Technology, Karlsruhe, Germany, in 2018. He is currently working toward the Ph.D. degree at the University of Edinburgh, U.K. His main research interest includes digital modulation techniques and visible light communication..

Harald Haas (FREng FRSE FIEEE FIET) received the Ph.D. degree from The University of Edinburgh in 2001. He is a Distinguished Professor of Mobile Communications at the University of Strathclyde and the Director of the LiFi Research and Development Centre. He also set-up and co-founded pureLiFi Ltd which it currently serves as Chief Scientific Officer. He has authored over 550 conference and journal papers. Haas' main research interests are in optical wireless communications, hybrid optical wireless and RF communications, spatial modulation, and interference coordination in wireless networks. His team invented spatial modulation. He introduced LiFi to the public at an invited TED Global talk in 2011. LiFi was listed among the 50 best inventions in TIME Magazine in 2011. In 2016, he received the Outstanding Achievement Award from the International Solid State Lighting Alliance. In 2019 he was the recipient of the IEEE Vehicular Society James Evans Avant Garde Award. Haas was elected a Fellow of the Royal Society of Edinburgh (RSE) in 2017. In the same year, he received a Royal Society Wolfson Research Merit Award and was elevated to IEEE Fellow. In 2018 he received a three-year EPSRC Established Career Fellowship extension and was elected Fellow of the IET. Haas was elected Fellow of the Royal Academy of Engineering (FREng) in 2019.

Wasiu O. Popoola (S'05–A'12–M'13–SM'16) is currently a University Senior Lecturer and Deputy Director of Learning and Teaching at the School of Engineering, University of Edinburgh, U.K. He has published over 110 journal articles/conference articles/patent and over seven of those are invited articles. He also co-authored the book Optical Wireless Communications: System and Channel Modeling with MATLAB and many other book chapters. His primary research interests are digital and optical communications, including VLC, FSO, and fiber communications. One of his journal articles ranked No. 2 in terms of the number of full text downloads within IEEE Xplore, in 2008, from the hundreds of articles published by IET Optoelectronics, since 1980. Another article he co-authored with one of his Ph.D. students received the Best Poster Award at the 2016 IEEE ICSAE Conference. Popoola is a science communicator appearing in science festivals and on 'BBC Radio 5live Science' programme in Oct. 2017. His publications have over 5600 citations and an h-index of 32 on Google Scholar. He is a senior member of IEEE, an associate editor of the IEEE Access journal and a Fellow of the Higher Education Academy (FHEA). He was an Invited speaker at various events including the 2016 IEEE Photonics Society Summer Topicals.